Appendix: Properties of the cellular automaton model

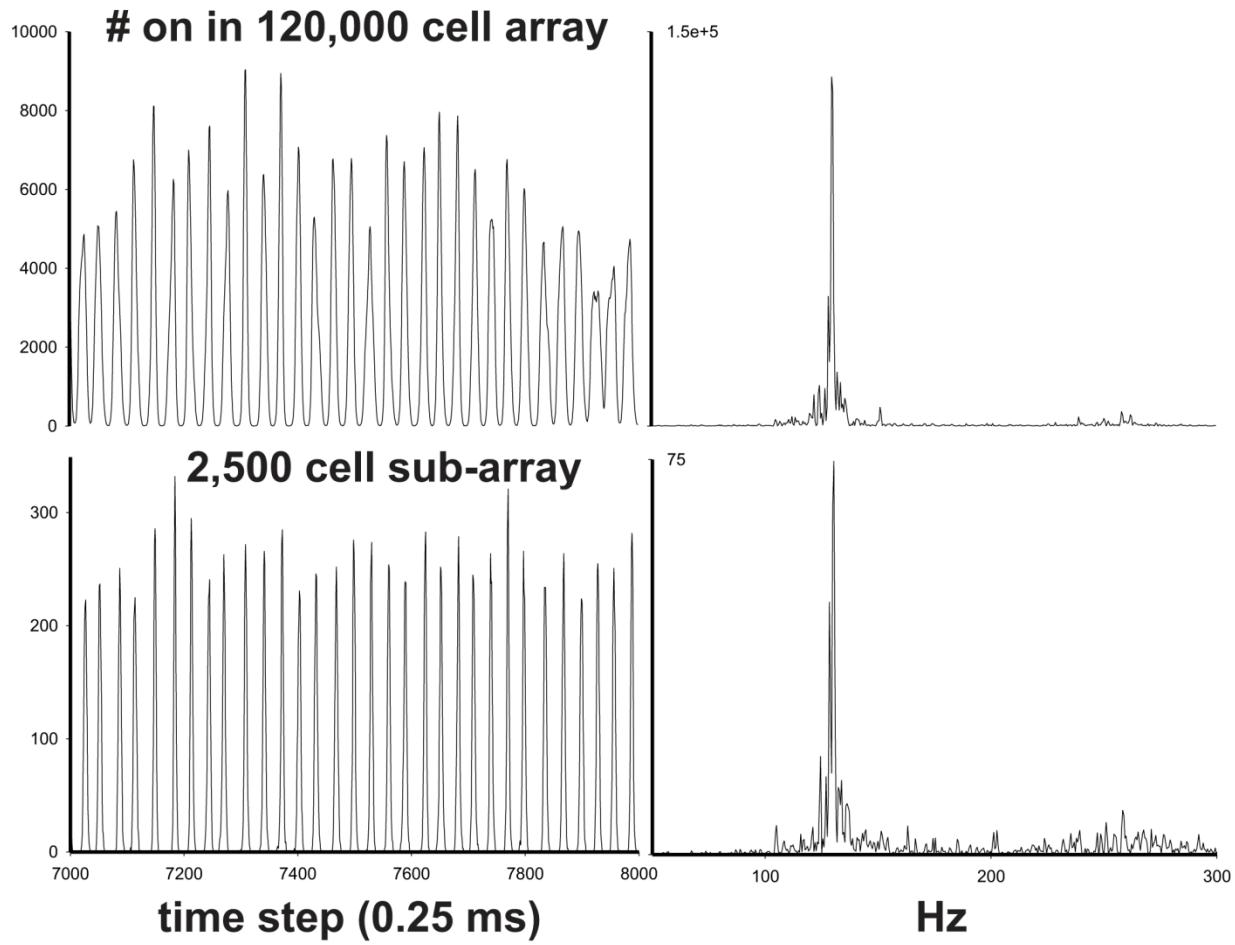

- Figure Appendix-1 -

Periodic network behavior. It is remarkable that network models with random structure and dynamics can exhibit periodic behavior (Traub et al., 1999; Lewis & Rinzel, 2000). Figure Appendix-1 shows that the present cellular automaton model exhibits the same sort of periodic behavior over a range of spatial scales. Such an observation eases worries about sampling ECoG data with relatively large electrodes, and with using a large number of electrodes – provided, that is, that one can assume that structural parameters corresponding to gap junction density and localization, and spontaneous spiking, are relatively constant over large expanses of cortex. Some insight into why this scale-independence of frequency exists is provided below, when the mechanism determining frequency is analyzed.

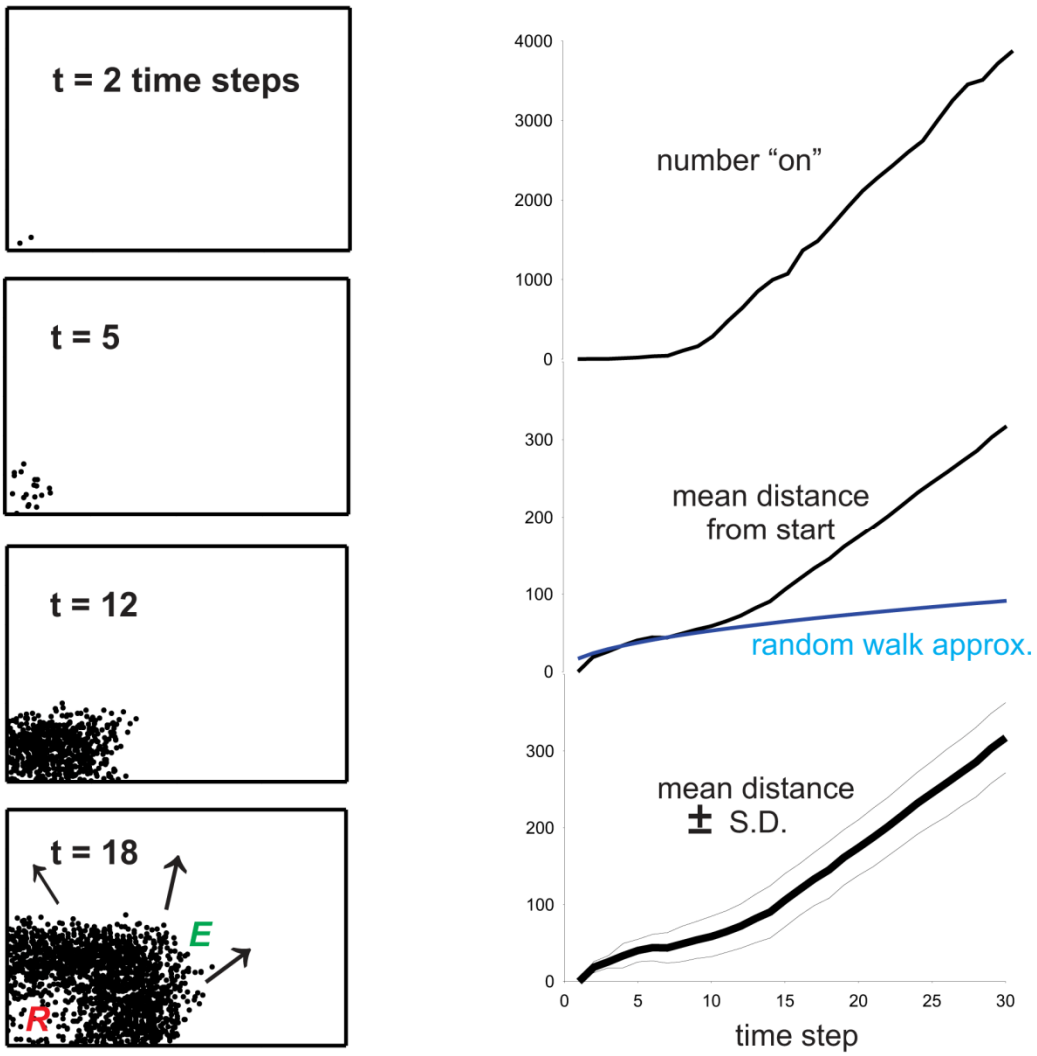

- Figure Appendix-2 -

Single waves grow and propagate linearly after an initial phase. Figure Appendix-2 illustrates the behavior of a single wave in the cellular automaton model, in the absence of noise (after the initial event starting the wave). The wave has two approximately separable phases. At first, the degree of activity is limited, attributable to the fact that the wave begins with a single firing cell, and each cell is coupled (on average) to very few others (a mean of only 1.33). When activity is sparse enough that each propagation can be imagined to occur independently of past events – that is, if we can assume that very few cells are occupied with firing or with being refractory, then it is possible to think of the cells firing at time t as resulting from a set of independent 2-dimensional random walks (Weisstein), starting at the initial site. The average step size for each random walk will be the expected value of radius r in a disk of radius c_r: this latter disk covers the territory in which there are possible connections from the starting site (at least, in the case of a starting site away from the boundaries). Thus, the average step size = $\int_0^{2\pi} \int_0^{c_r} r \, d\theta \, dr = 2\, c_r / 3$. The expected distance traveled at time t will then be $2\, c_r\, t^{1/2} / 3$, so that propagation only goes

as the square root of time. On the other hand, as shown by Lewis and Rinzel (2000) and confirmed here empirically (i.e. with many simulations), growth and propagation switch to being linear in time, with the wave having a refractory "wake" behind it, and propagation proceeding into excitable "territory" ahead of the wave – provided c_r is not too large; in the very large 3D model, the threshold value of c_r is about 50 lattice spacings: wave propagation occurs, that is, when $c_r \leq 50$. Remarkably, the wave thickness remains approximately constant over time, for reasons that remain to be explored.

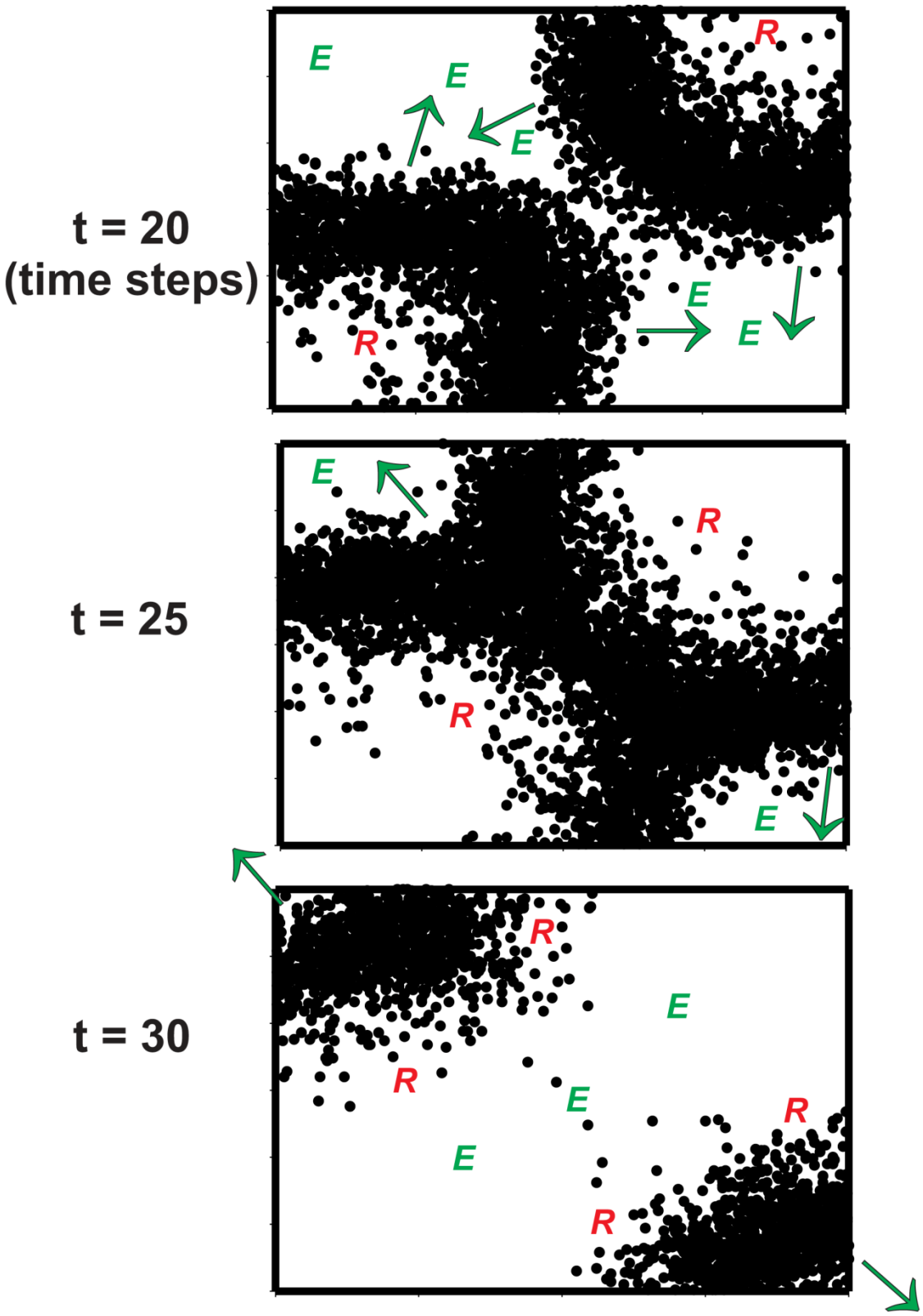

- Figure Appendix-3 -

Coalescence of waves, followed by propagation in different directions. Figure Appendix-3 illustrates for our a particular model a principle shown by Lewis and Rinzel (2000): two waves, propagating toward each other and meeting, will each have a refractory "wake". Therefore, the two waves can not pass through each other – unlike waves propagating across a pond after two stones have been dropped simultaneously into the pond at different spots. Instead, the waves are forced to propagate in different directions (in the illustrated case, roughly at right angles to the original directions of propagation), into "virgin territory", where excitable cells are available.

A formula for estimating the oscillation period in the cellular automaton, when p_{spon} is small. We have seen that the CA model generates arcing and circular wavefronts that expand away from a spontaneous firing. Suppose such a wavefront is expanding from the interior of a large array and a wavefront meets it *from the outside*. Such a collision will result in coalescence and continued expansion (Figure Appendix-3); it will not contribute to periodicity of the overall activity. On the other hand, a new wavefront originating *on the inside* can never meet the original wavefront: the wavefronts propagate at the same velocity and one can not catch up with the other; even if it could catch up, the refractory wake will prevent coalescence. Thus, the period will be determined by the mean rate at which wavefronts arise, from spontaneous events, *within* other wavefronts. [Note that this rate is scale-free, if the network is large enough: spontaneous events within one expanding wave occur independently of spontaneous events within other expanding waves – hence the observation in Figure Appendix-1 that oscillation frequency is independent of network scale.]

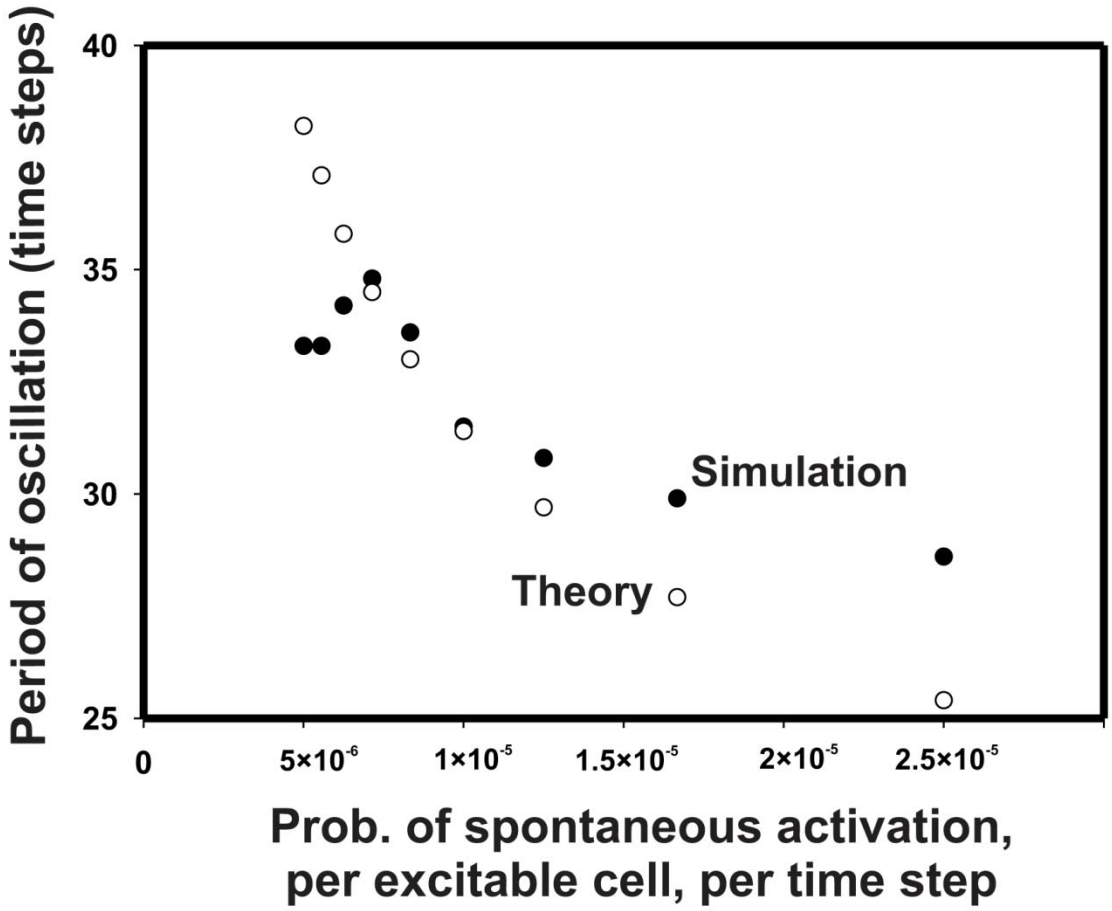

- Figure Appendix-4 -

We can estimate this rate if p_{spon} is small enough so that it is improbable that two spontaneous events occur within a single expanding wavefront; and if we make the approximation that wave propagation is strictly linear (which is not actually true at short times after a spontaneous event – Figure Appendix-2). Let t be the time step, r the number of refractory steps (15 for the present model), and a be the number of cells the wave grows by in each time step (a = 185 in Figure Appendix-2). [The quantity a will in turn depend on structural parameters <i> and c_r in a manner to be determined in a later paper.] The number of excitable cells *within* an expanding wave at time t after one spontaneous event (i.e. the number of cells in which a new wave might start) will be the greater of 0 and

$a + 2a + 3a + ... + (t-r)a \sim a(t-r)^2 / 2$. The expected number of spontaneous events within the wave at time t will be $\sim p_{spon} \times a(t-r)^2 / 2$, once $t > r$. If we set the expected number of spontaneous events = 1, we obtain a quadratic equation in t, the larger (i.e. physical) solution of which is $t = r + (1 / 2\, a\, p_{spon})^{1/2}$. Thus, we estimate the period as equal to the intrinsic refractoriness plus a term that depends on the inverse square root of certain structural parameters. Figure Appendix-4 shows a range of p_{spon} for which this formula gives reasonable estimates of

the period. Of course, as p_{spon} becomes large enough, then it becomes increasingly likely that two or more events occur within a wavefront, and the formula will diverge from simulation results.

References for Appendix

Lewis TJ, Rinzel J (2000) Self-organized synchronous oscillations in a network of excitable cells coupled by gap junctions. *Network: Comput. Neural Syst*. 11: 299-320.

Traub RD, Schmitz D, Jefferys JGR, Draguhn A (1999) High-frequency population oscillations are predicted to occur in hippocampal pyramidal neuronal networks interconnected by axoaxonal gap junctions. *Neuroscience* 92: 407-426.

Weisstein EW. Random Walk – 2-Dimensional. In *MathWorld* – A Wolfram Web Resource. http://mathworld.wolfram.com/RandomWalk2-Dimensional.html.

Appendix Figure Legends

Figure Appendix 1. Local random connectivity is consistent with periodic network behavior that is scale-invariant. Simulation was of a 120,000 cell (400 × 300) cellular automaton model, with mean index <i> = 1.33 and $p_{spon} = 1.25\times10^{-5}$ (as in Fig. 2), and $c_r = 25$ lattice spacings. The frequency of net activity in the whole array was the same as in a square sub-array that was 1/48 the size of the original array. Power spectra were computed from 8,192 data points. (When the array size was increased 4-fold, other parameters being kept the same, the frequency also did not change – not shown). In spite of the frequency invariance, complex patterns of spatial activity are nevertheless occurring (see below). This simulation also suggests that using subdural grid electrodes, as opposed to microelectrodes, may not give a misleading measurement of frequency, provided oscillations are occurring in a sufficient volume of tissue.

Figure Appendix 2. Growth and wave propagation from a single cell being "on", in the absence of spontaneous activity: the initial growth can be approximated by a 2-dimensional random walk, but then a wave forms that grows linearly in time (until it hits an array boundary), and that moves linearly in time. Simulation was from a cellular automaton model as in Figure Appendix 1, but with $p_{spon} = 0$, and with a single cell in the lower left corner set to be "on" initially. In the frames at left, "on" cells are indicated by black dots. There is a refractory "wake" behind the wave (red R), and the wave propagates into the territory of excitable cells (green E) (c.f. Lewis & Rinzel, 2000). Graphs at the right characterize wave growth and propagation. The upper graph shows that growth is linear after about 10 time steps (over the interval t = 15 to 30, the slope is 185 cells/time step, $r^2 = 1.00$). Likewise, the wave moves at constant velocity after about 15 time steps (middle graph: over the interval t = 15 – 30, the velocity is 14 lattice spacings/time step, $r^2 = 1.00$). The blue curve shows propagation expected for a 2-dimensional random walk

with step size equal to 2/3 × c_r (this is the expected value of a "jump" – see text); in a random walk, expected distance grows with $\sqrt{time}$ rather than linearly in time. The bottom graph shows that the thickness of the propagating wave remains approximately constant.

Figure Appendix 3. Coalescence of two propagating waves in the cellular automaton model (see also (Lewis & Rinzel, 2000). Simulation is of spontaneous activity with parameters as in Appendix Figure 1, with 120,000 cells in a 400 × 300 array. In the case shown, at t = 20, one wave originated near the lower left corner, and is propagating upwards and to the right, leaving a refractory wake behind it (red R). The other wave originated near the upper right corner and is propagating downward and to the left; it also leaves a refractory wake (red R). Each wave is propagating into regions of excitable cells (green E). At t = 25, the waves meet, near the center of the array. Because of the refractory wakes, they can not pass through each other, but instead start to propagate toward the excitable corners of the system: the upper left, and lower right. At t = 30, the waves dissipate across the corners of the array. We propose that this type of wave interaction characterizes pre-seizure VFO in cortex.

Figure Appendix 4. Comparison of formula for network oscillation period with simulation data. For derivation of the formula, see text. Simulations were run in a cellular automaton model with 120,000 cells (400 × 300 array), with mean index <i> = 1.33 and c_r = 25. p_{spon} (the abscissa) was varied. The theoretical prediction is quite accurate for small p_{spon}, although when p_{spon} is very small, the accuracy of prediction is limited by statistical fluctuations. The theory starts to diverge from simulation results as p_{spon} becomes large enough; we attribute this to the occurrence of more than one spontaneous event within expanding waves, contrary to the assumption for the theory.